Proceedings 10th NUMGE 2023
10th European Conference on Numerical Methods in Geotechnical Engineering
Zdravkovic L, Kontoe S, Taborda DMG, Tsiampousi A (eds)

https://doi.org/10.53243/NUMGE2023-234

Imprecise moment-independent global sensitivity analysis of rock slope using Bayesian multi-model inference

A. Kumar[1], G. Tiwari[1]

[1]*Department of Civil Engineering, Indian Institute of Technology, Kanpur, India*

ABSTRACT: Traditional global sensitivity analysis (GSA) provides the relative importance of uncertain rock input properties towards rock structure response, given their best-fit probability distribution model and parameters. However, the availability of limited experimental data for the rock properties due to in-situ and laboratory testing complexities affects the model type and parameter accuracy. This study presents an augmented probabilistic methodology by coupling the multi-model and traditional Bayesian inference. The methodology incorporates the uncertainties associated with both the model type and parameter for estimating Borgonovo's moment-independent sensitivity indices. The methodology is demonstrated for a rock slope having the potential of stress-controlled failure. It is concluded that the methodology results in imprecise sensitivity indices providing a measure of confidence in sensitivity estimates when limited data are available for properties. Further, the comparative analysis with traditional GSA concluded the superiority of the proposed methodology as it treats the uncertainties in both model type and parameters.

Keywords: Bayesian inference; multi model inference; statistical uncertainty; global sensitivity analysis; limited data

1 INTRODUCTION

In rock engineering practices, the importance of rock properties and impact of their associated uncertainties on the rock structure response is often required, such as in efficient resource allocation, responsible decision-making, dimensional reduction etc (Kumar and Tiwari, 2022; Pandit et al., 2023, 2018). Sensitivity analysis methods are used to facilitate this in the literature. Sensitivity analysis methods are broadly categorized as: local (LSA) and global (GSA). LSA refer to local sensitivity of inputs around a nominal point of interest. In contrast, GSA estimates the effects of entire input space on the response. Widely used Sobol's GSA considers the change in the variance (i.e., a statistical moment) of response for a specific value of input to estimate its sensitivity. Other class of GSA includes moment-independent method, proposed by Borgonovo (2007), considers the probability distribution of response to map the sensitivity of inputs. Adoption of Borgonovo's moment-independent GSA in rock engineering domain has been limited (Pandit et al., 2023; Xu et al., 2020).

Monte Carlo simulation (MCS) based routines of Borgonovo's GSA require statistical characteristics, i.e., probability distribution model type and its parameters, of the input properties (Borgonovo, 2007; Pandit et al., 2023). Hence, accurate estimation of the statistical characteristics of properties is a must, which in turn depends upon the quantity of the laboratory and in-situ investigation data. However, datasets to characterize the properties are more often sparsely available for rock mechanics projects due to high costs in testing, practical difficulties, sample preparation etc (Kumar and Tiwari, 2022; Pandit et al., 2018). In such situations, the statistical characteristics themselves become uncertain (i.e., statistical uncertainty), and the traditional GSA utilizing these uncertain statistical characteristics may lead to inaccurate estimates of sensitivity indices.

To improve on traditional GSA, this study presents an imprecise GSA methodology to account for the complete statistical uncertainty associated with probability model type and parameters arising from the limited data of rock properties. Within the methodology, the multi-model inference (MMI) is first utilized to identify a set of plausible probability models for a property to incorporate the uncertainty associated with the model type. Then, Bayesian inference is employed for each model, quantifying the uncertainty associated with model parameters. By applying the proposed approach to a natural rock slope case study prone to stress-controlled failure, it is demonstrated that the proposed methodology can conveniently facilitate the GSA of rock slopes with limited data of properties.

2 DETAILS OF THE COMPONENTS OF METHODOLOGY

In this section, the major components of the proposed methodology, are presented.

2.1 *Borgonovo's moment-independent sensitivity analysis*

Moment-independent GSA considers the change in the entire probability distribution of output in contrast to any particular moment, such as variance for Sobol's GSA, to evaluate inputs sensitivities. The basic idea behind the method is described in Figure 1. The unconditional model output density $f_Y(y)$ is obtained with varying all model inputs $\boldsymbol{X}$ as per their distributions and the conditional density $f_{Y|X_i}(y)$ by keeping the model input X_i constant. Sensitivity index of X_i can be evaluated by measuring the separation area between the unconditional and conditional model output densities (Borgonovo, 2007).

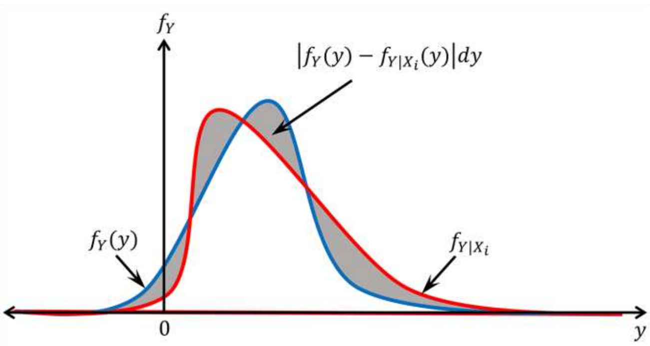

Figure 1. Illustration of the separation area required for the estimation of Borgonovo's sensitivity indices

Mathematically, the sensitivity of a input X_i based on Borgonovo's method can be given as below.

$$\delta_i = \frac{1}{2}\int_{D_{X_i}} f_{X_i}(x_i) \int_{D_Y} \left| f_Y(y) - f_{Y|X_i}(y) \right| dy dx_i \quad (1)$$

where δ_i represents the sensitivity measure of X_i; $f_Y(y)$ is the PDF of Y; $f_{Y|X_i}(y)$ is conditional PDF of Y; D_{X_i} and D_Y represent entire domains of X_i and Y, respectively.

In this study, Borgonovo's analysis was performed via a histogram-based approximation based on MCS due to its robustness and simplicity (Pandit et al., 2023). The steps involved in the method are shown below:

1. Generate a random realization $\boldsymbol{x}$ of size N for input random vector $\boldsymbol{X} = (X_1, X_2, \dots, X_d)$ with d variables based on their probability distributions $f_{X_i}(x_i)$.

$$\boldsymbol{x} = \begin{bmatrix} x_1^{(1)} & x_1^{(2)} & \dots & x_1^{(N)} \\ x_2^{(1)} & x_2^{(2)} & \dots & x_2^{(N)} \\ \vdots & \vdots & \ddots & \vdots \\ x_d^{(1)} & x_d^{(2)} & \dots & x_d^{(N)} \end{bmatrix} = \left(\boldsymbol{x}^{(1)}, \boldsymbol{x}^{(2)}, \dots, \boldsymbol{x}^{(N)}\right) \quad (2)$$

2. Evaluate the response $G(\cdot)$ for random realizations of $\boldsymbol{x}$, i.e., $Y = (y_1, y_2, \dots, y_N) = G\left(\boldsymbol{x}^{(1)}, \boldsymbol{x}^{(2)}, \dots, \boldsymbol{x}^{(N)}\right)$ and estimate the unconditional PDF $f_Y(y)$ via the normalized histogram, to give probability values, with a predefined number of bins n_y as given below.

$$\hat{f}_Y = \left(\hat{f}_Y^{(1)}(y), \hat{f}_Y^{(2)}(y), \dots, \hat{f}_Y^{(n_y)}(y)\right) \quad (3)$$

3. Divide $\boldsymbol{x} = (\boldsymbol{x}^{(1)}, \boldsymbol{x}^{(2)}, \dots, \boldsymbol{x}^{(N)})$ into n_x classes (subsets) for input X_i under consideration. Each of the n_x classes (C_{n_x}) is defined by its lower and upper limits $\{l_q, u_q\}$ with $l_q < u_q$, $q \in \{1,2,\dots,n_x\}$. Class C_{n_x} include all samples of $\boldsymbol{x}^{(j)}, j \in \{1,2,\dots,N\}$ whose realizations of X_i, i.e., $x_i^{(j)}$ lies in the interval $\{l_q, u_q\}$, i.e., $C_{n_x} = \left\{x^{(j)}: l_q \le x_i^{(j)} \le u_q\right\}$. The probability $P\left(\boldsymbol{x}^{(j)} \in C_{n_x}\right)$ is $\frac{1}{n_x}$ for sufficiently large N.

4. Evaluate the response values corresponding to each class, i.e., $G\left(\boldsymbol{x}^{(j)}\right), \boldsymbol{x}^{(j)} \in C_{n_x}$, and estimate the distribution of Y in each class ($\hat{f}^{(C_{n_x},t)}{}_{Y|X_i}(y)$) via the normalized histogram with n_y bins approximately as $\hat{f}^{(C_{n_x},t)}{}_{Y|X_i}(y) = \left(\hat{f}^{(1,t)}{}_{Y|X_i}(y), \dots, \hat{f}^{(n_x,t)}{}_{Y|X_i}(y)\right)$, where $t \in \{1,2,\dots,n_y\}$.

5. Estimate the δ_i in accordance with the integral in Equation (1), as given below.

$$\delta_i = \frac{1}{2}\left(\sum_{j=1}^{n_x} \frac{1}{n_x}\left(\sum_{k=1}^{n_y}\left|\hat{f}_Y^{(k)}(y) - \hat{f}^{(j,k)}{}_{Y|X_i}(y)\right|\right)\right) \quad (4)$$

6. Repeat steps 3 to 5 for each X_i, $i = 1, 2, \dots, d$ and estimate the corresponding δ_i.

The above algorithm is implemented in MATLAB.

2.2 *Multi-model inference (MMI)*

MMI quantifies the uncertainty in probability model identification for a limited data $\boldsymbol{D}$ of the property. Instead of a single best-fit model to represent dataset at-hand, MMI identifies the multiple competing models $\boldsymbol{M} = \{M_1, M_2, \dots, M_{N_d}\}$ to be considered into the analysis (Burnham and Anderson, 2004; Zhang and Shields, 2018). MMI employs the Akaike Information Criterion (AIC) for model selection. Model with the lowest AIC value is considered to be best fit to represent the data. For small datasets, an extension of the AIC, AIC_c has been developed, as given below.

$$AIC_c^{(i)} = -2\log\left(p(\boldsymbol{D}|\widehat{\boldsymbol{\theta}}, M_i)\right) + 2K + \frac{2K(K+1)}{n-K-1} \quad (5)$$

where $p\left(\boldsymbol{D}|\widehat{\boldsymbol{\theta}}, M_i\right)$ is the likelihood function given maximum likelihood estimate of the parameters $\widehat{\boldsymbol{\theta}}$, K is the number of candidate model M_i parameters, and n is the number of observations in the dataset. AIC_c converges to AIC for large n. AIC_c is utilized for multi-model selection in this study. Once the AIC_c value is known for each model in the candidate set, AIC_c difference values (Δ_A) can be calculated to interpret the ranking of candidate models as given below (Burnham and Anderson, 2004):

$$\Delta_A^{(i)} = AIC_C^{(i)} - AIC_C^{min} \quad (6)$$

where AIC_C^{min} is the minimum of the different $AIC_C^{(i)}$ values corresponding to $\boldsymbol{M} = \{M_1, M_2, \dots, M_{N_d}\}$. This transformation forces the best model to have $\Delta_A^{(i)} = 0$ and all other models have positive values. Further, the likelihood of the model M_i can be expressed as $\exp\left(-\frac{1}{2}\Delta_A^{(i)}\right)$ and by normalizing these likelihoods the model probability values w_i can be estimated as below.

$$w_i = p(M_i|d) = \frac{\exp\left(-\frac{1}{2}\Delta_A^{(i)}\right)}{\sum_{m=1}^{N}\exp\left(-\frac{1}{2}\Delta_A^{(m)}\right)} \quad (7)$$

The larger the w_i, the more plausible is model as being the best fit model to dataset $\boldsymbol{D}$.

2.3 Bayesian inference

Bayesian inference enables to quantify the uncertainty associated with parameters for probability model M_i. Within the framework, model parameters $\boldsymbol{\theta}$ are treated as a random variable by combining prior knowledge, in terms of the prior distribution $p(\boldsymbol{\theta}; M_i)$, with site-specific observation data $\boldsymbol{D}$, in terms of the likelihood function $p(\boldsymbol{D}|\boldsymbol{\theta}, M_i)$. The posterior distribution $p(\boldsymbol{\theta}|\boldsymbol{D}, M_i)$, i.e., the updated probability density function of parameters $\boldsymbol{\theta}$ according to Bayes rule can be written as (Aladejare and Wang, 2018; Contreras et al., 2018)

$$p(\boldsymbol{\theta}|\boldsymbol{D}, M_i) = \frac{p(\boldsymbol{D}|\boldsymbol{\theta}, M_i)p(\boldsymbol{\theta}; M_i)}{p(\boldsymbol{D}; M_i)} \quad (8)$$

where $p(\boldsymbol{D}; M_i)$ is the normalizing factor that makes the posterior distribution to integrate to one. The Markov Chain Monte Carlo (MCMC) simulation technique can be employed to generate a sequence of random samples from the posterior $p(\boldsymbol{\theta}|\boldsymbol{D}, M_i)$. Details of the Metropolis-Hasting MCMC technique employed in this study can be found in the literature (Aladejare and Wang, 2018).

3 PROPOSED IMPRECISE GLOBAL SENSITIVITY ANALYSIS (IGSA)

This section describes the proposed IGSA methodology wherein the complete statistical uncertainty, i.e., uncertainty associated with probability model types and parameters, can be considered in estimation the sensitivity indices of rock properties. The IGSA first utilizes the MMI approach to identify the plausible set of probability distribution models representative of the limited sized dataset of rock properties. Next, the Bayesian inference is employed for each plausible model to quantify the model parameters uncertainty. Finally, this is propagated via the traditional GSA on the sensitivity indices. The steps involved in the proposed IGSA are as follows:

Step 1 Derivation of performance function (PF): derive the PF using analytical methods or surrogate modeling in-case the PF is not available in the explicit form.

Step 2 Identification of plausible models: compute AIC_c and probability w_i for the candidate probability models and identify the plausible set of models for the rock properties, as described in section 2.2.

Step 3 Estimation of posterior model parameters: estimate the updated/posterior model parameters for each plausible model, i.e., $p(\boldsymbol{\theta}|\boldsymbol{D}, \boldsymbol{M})$, through MH-MCMC, as described in section 2.3.

Step 4 Establishment of a model ensemble: establish an ensemble with finite but large models for each rock property, where the number of times a model is selected is proportional to its probability value w_i. The model parameters are then randomly drawn from the posterior parameter density, estimated in the previous step.

Step 5 Estimation of imprecise Borgonovo's sensitivity indices: estimate the Borgonovo's moment-independent indices via the MCSs algorithm by generating N random realizations (section 2) corresponding to each model in the established model ensemble established in the previous step and obtain the statistics of the sensitivity indices, i.e., mean, coefficient of variation (COV) and PDFs for all rock properties.

A MATLAB code is written to implement all the above steps sequentially when analyzing the stability of rock structures.

4 CASE STUDY

To demonstrate the proposed IGSA methodology, a gold mine rock slope situated in the Karnataka state in India (Pandit et al., 2018) was considered in the study. Geological details of the slope can be found in the study by Pandit et al. (2018). The slope was modelled using the finite difference method (FDM) in the FLAC-2D software. Figure 2 shows the established numerical model. Rock mass along the slope is assumed to follow elastic-perfectly plastic behavior with Hoek-Brown (H-B) criterion. The factor of safety (FOS) of the slope was estimated using strength reduction technique by considering a locally approximated Mohr-Coulomb model. Intact rock properties (i.e., H-B strength parameter m_i, uniaxial compressive strength UCS, and elastic modulus E_i), and geological strength index (GSI) were estimated using International Society of Rock Mechanics (ISRM) suggested field and laboratory testing methods. Table 1 depicts the statistics of the intact rock properties and GSI. The dataset contains only 22 investigations (Pandit et al., 2018), which is statistically small. Hence, the proposed methodology was used to evaluate the imprecision in sensitivity indices of properties.

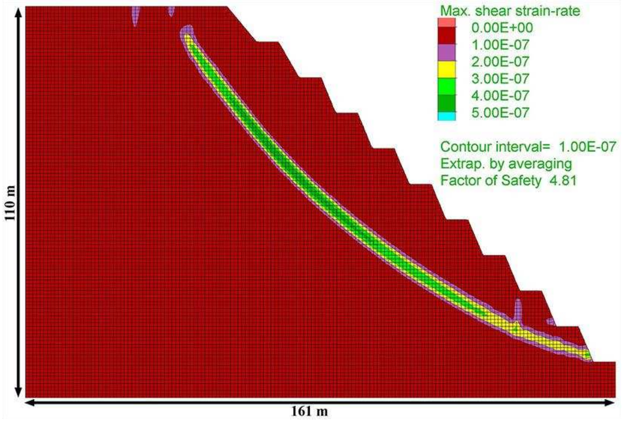

Figure 2. Typical FDM numerical model of the slope prepared in FLAC-2D

Table 1. Statistic of intact rock properties and GSI (Pandit et al., 2018)

Property	Mean	COV
UCS (MPa)	65.45	0.59
GSI	49.32	0.30
m_i	17.11	0.49
E_i (GPa)	9.19	0.55

Step 1 Derivation of performance function (PF): since FDM numerical model was used to model slope stability that lacks explicit relation for the PF (i.e., FOS), the radial basis function (RBF) Response Surface Method (RSM) was used in this study to construct surrogate PF. Mathematical details of the RBF RSM construction and FOS estimation can be found in study by Pandit et al. (2018). The surrogate relationship was constructed such that it takes intact rock properties and GSI as inputs. The reason is that the intact rock properties are estimated in the laboratory and GSI in the field, which are later reduced to represent rock mass properties based on GSI classification system (Hoek et al., 2002; Hoek and Diederichs, 2006). Hence, it was required to evaluate the sensitivities of directly measurable properties for efficient allocation of the available laboratory and in situ resources. The RBF RSM was constructed using 200 Latin Hypercube sampling points generated as per statistics of input properties, and its Nash–Stucliffe Efficiency using 50 off-sampling points was estimated to be 0.9071, which corresponds to *very good* accuracy (Pandit et al., 2018).

Step 2 Identification of plausible models: a candidate model set was first chosen for each rock property. Since rock properties cannot have negative values, probability models which support over the positive real line were considered as candidate models. The w_i for each candidate model in set was estimated. Table 2 shows the candidate model set for all properties along with estimated w_i. It was observed that multiple models have an almost similar probability of representing the data. This can be attributed to the fact that identifying a best-fit model is not feasible from the small dataset. Hence, except the Lognormal and Inverse Gaussian model for GSI, all other candidate models for rock properties were considered as plausible models for further analysis.

Step 3 Estimation of posterior model parameters: once the plausible models were known, the posterior model parameters for each plausible model $p(\boldsymbol{\theta}|\boldsymbol{D},\boldsymbol{M})$ are estimated through Bayesian inference utilizing MH-MCMC sampling (section 3). Uniform prior distribution $p(\boldsymbol{\theta};\boldsymbol{M})$ was assumed to represent the prior information of model parameters. The ranges of mean and COV for the rock properties were adopted from the literature (Aladejare and Wang, 2017), as in Table 3. A total of 100,000 random samples from $p(\boldsymbol{\theta}|\boldsymbol{D},\boldsymbol{M})$ were generated with discarding the initial 10,000 samples as burn-in samples. This was performed for each input property, i.e., m_i, UCS, E_i and GSI. Figure 3 shows the joint PDFs of the posterior model parameters for the plausible models of UCS. Red points show the model parameter value estimated from limited in-situ data, and the contour area indicates model parameter uncertainty.

Step 4 Establishment of a model ensemble: a model ensemble with a total of 10,000 models for each rock property, i.e., m_i, UCS, E_i and GSI was established (section 3). Figure 4 shows the constructed model ensembles for UCS (due to length limitation of the paper). The model ensembles represented the complete statistical uncertainty associated with the probabilistic characterization of rock properties with limited data.

Table 2. Candidate marginal models and their corresponding AIC_c and probability values $\boldsymbol{w}$ for rock properties

Candidate model	$\boldsymbol{UCS}$		$\boldsymbol{GSI}$		$\boldsymbol{m_i}$		$\boldsymbol{E_i}$	
	$\boldsymbol{AIC_c}$	$\boldsymbol{w}$	$\boldsymbol{AIC_c}$	$\boldsymbol{w}$	$\boldsymbol{AIC_c}$	$\boldsymbol{w}$	$\boldsymbol{AIC_c}$	$\boldsymbol{w}$
Lognormal	223.899	0.136	201.106	**0.000**	160.861	0.085	134.942	0.143
Weibull	222.963	0.217	185.516	0.873	158.285	0.311	134.242	0.203
Gamma	222.893	0.224	194.221	0.011	159.391	0.179	134.105	0.218
Inverse Gaussian	223.794	0.143	204.388	**0.000**	160.460	0.105	134.699	0.162
Nakagami	223.029	0.210	189.866	0.099	158.450	0.286	134.254	0.202
Loglogistic	225.201	0.071	193.572	0.015	162.879	0.031	136.377	0.070

Text in bold represents the candidate marginal models with approximately zero $\boldsymbol{w}$ values

Table 3. Prior information for the rock properties (Aladejare and Wang, 2017)

Property	Mean	COV
$\boldsymbol{UCS}$ (MPa)	4.4–264	0.004–1.096
$\boldsymbol{GSI}$	22.60–60.40	0.171–0.27
$\boldsymbol{m_i}$	4–21	0.142–0.275
$\boldsymbol{E_i}$ (GPa)	0.59–73.17	0.07–1.281

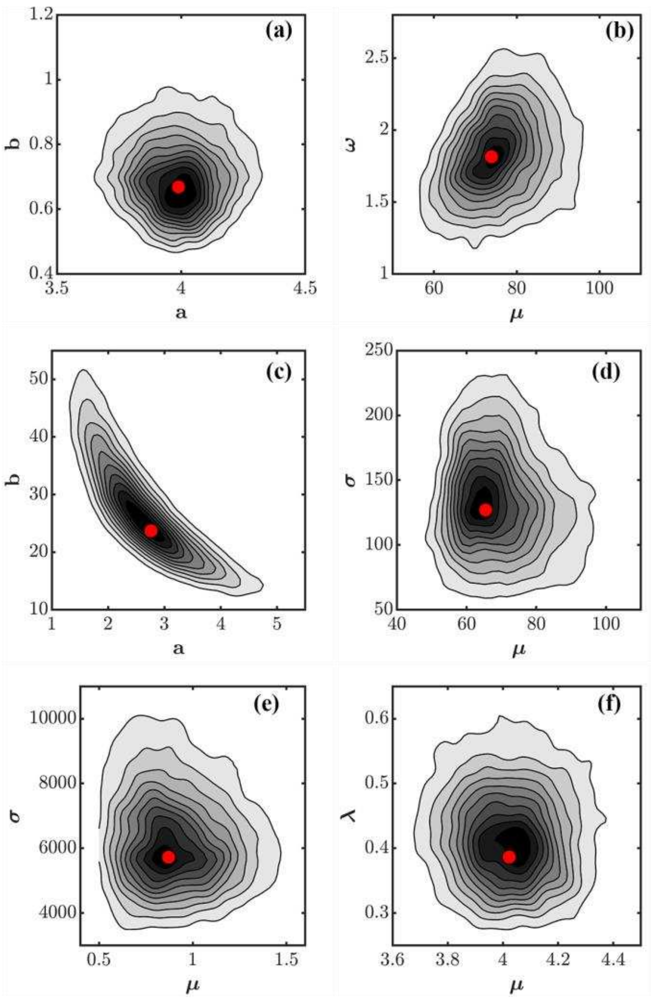

Figure 3. Joint PDFs of posterior model parameters of the plausible models (a) Lognormal, (b) Weibull, (c) Gamma,(d) Inverse Gaussian, (e) Nakagami, and (f) Loglogistic of UCS

Step 5 Estimation of imprecise Borgonovo's sensitivity indices: in this step, statistical uncertainty associated with rock properties was propagated on Borgonovo's sensitivity indices. For this, Borgonovo's sensitivity analysis was performed sequentially for all 10,000 models in an ensemble for each property. Sensitivity indices were estimated by generating N=100,000 random realizations for each property with n_x and n_y being taken as 30 (section 2.1). The FOSs required to evaluate the sensitivity indices were estimated using the RBF RSM function constructed in Step 1. Following this, in total 10,000 values of sensitivity indices for all properties were obtained. Figure 5 shows the PDF of the sensitivity indices along with their point estimate from the traditional Brogonovo's analysis neglection statistical uncertainty. The distribution indicates the imprecision arising from both model type and parameter estimation with the limited property data.

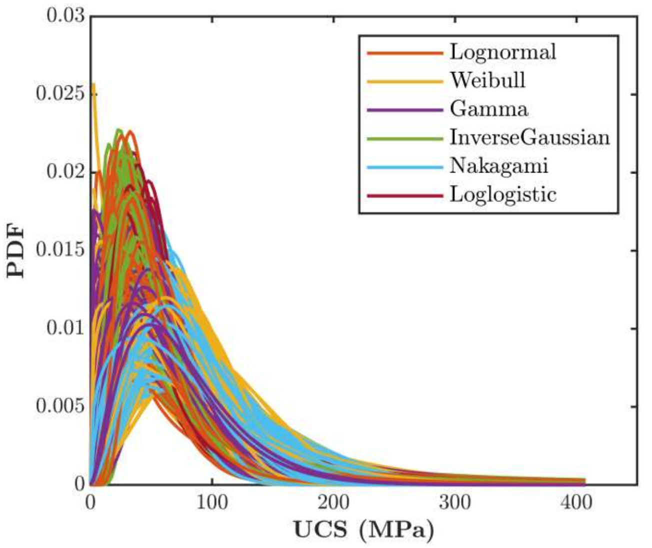

Figure 4. Model ensemble with a total of 10,000 models established for UCS

UCS and GSI were observed to be more sensitive towards FOS of the slope with their sensitivity indices ranging in the intervals (95% confidence interval (CI)) [0.1204–0.3646], and [0.2293–0.5362], respectively. m_i and E_i showed lesser sensitivities with sensitivity indices ranging in the interval [0.0364–0.1618] and [0.0294–0.0686], respectively. Properties with higher sensitivities, i.e., UCS and GSI have wider CIs compared to the lesser sensitive ones. However, to ascertain the most sensitive property, the precise individual importance ranking of rock properties was not possible due to significant overlapping CIs of sensitivity indices (Figure 5).

5 CONCLUSIONS

This study presented an imprecise Borgonovo's moment-independent sensitivity analysis methodology wherein the effect of uncertainties associated with both probability model types and parameters arising from limited data of rock properties can be considered. The methodology quantifies the uncertainties in the probability model types and parameters by coupling the MMI and Bayesian inference. A mine rock slope potential to stress-controlled failure was considered to demonstrate the methodology. The methodology provides a distribution/confidence interval of sensitivity indices by considering the effect of statistical uncertainty instead of a point estimate from traditional GSA. The Coefficient of Variation (COV) of sensitivity indices from the proposed methodology ranged from 15-29%, indicating the significant impact of statistical uncertainty on the sensitivity indices. Based on the CIs of sensitivity indices, rock properties were grouped into two categories a) highly sensitive, i.e., UCS and GSI

and b) lesser sensitive, i.e., m_i and E_i, and their precise individual ranking was not feasible due to overlapping CIs. Although the proposed methodology is more computationally demanding than traditional GSA, it provides a way to account for the impact of statistical uncertainty in estimating sensitivity indices of rock properties that cannot be quantified using traditional GSA. Hence, the proposed methodology was concluded as superior to traditional GSA.

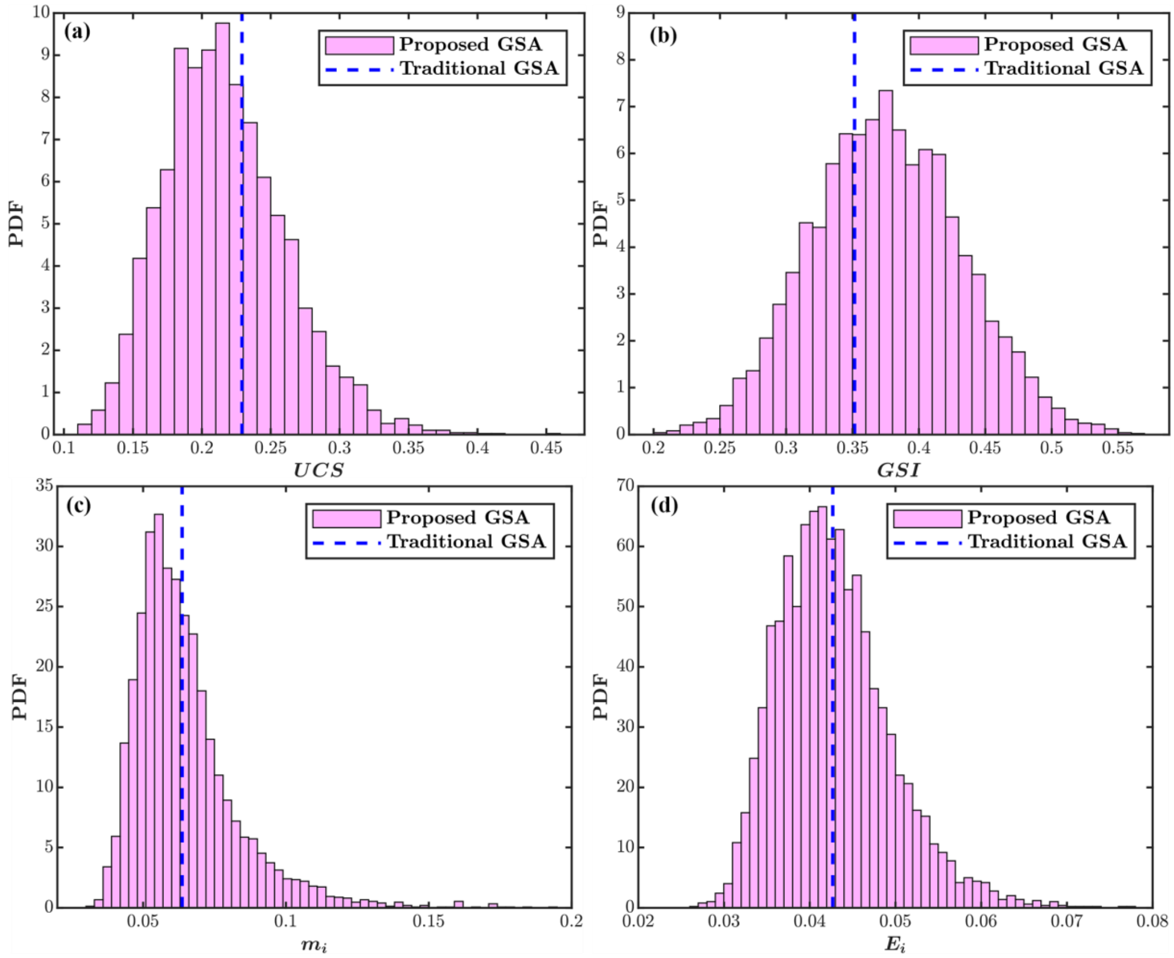

Figure 5. The PDFs of Borgonovo's sensitivity indices for (a) UCS, (b) GSI, (c) m_i, and (d) E_i

6 REFERENCES

Aladejare, A.E., Wang, Y. 2017. Evaluation of rock property variability *Georisk* **11**, 22–41.

Aladejare, A.E., Wang, Y. 2018. Influence of rock property correlation on reliability analysis of rock slope stability: From property characterization to reliability analysis *Geoscience Frontiers* **9**, 1639–48.

Borgonovo, E. 2007. A new uncertainty importance measure *Reliab Eng Syst Saf* **92**, 771–84.

Burnham, K.P., Anderson, D.R. 2004. Multimodel inference: Understanding AIC and BIC in model selection *Sociol Methods Res* **33**, 261–304.

Contreras, L.F., Brown, E.T., Ruest, M. 2018. Bayesian data analysis to quantify the uncertainty of intact rock strength *Journal of Rock Mechanics and Geotechnical Engineering* **10**, 11–31.

Hoek, E., Carranza, C., Corkum, B., 2002. Hoek-brown failure criterion – 2002 edition. *Proceedings of NARMS-Tac* **1**, 267–273.

Hoek, E., Diederichs, M.S., 2006. Empirical estimation of rock mass modulus. *International Journal of Rock Mechanics and Mining Sciences* **43**, 203–215.

Kumar, A., Tiwari, G. 2022. Jackknife based generalized resampling reliability approach for rock slopes and tunnels stability analyses with limited data: Theory and applications *Journal of Rock Mechanics and Geotechnical Engineering* **14**, 714–30.

Pandit, B., Kumar, A., Tiwari, G. 2023. Assessing the applicability of local and global sensitivity approaches and their practical utility for probabilistic analysis of rock slope stability problems: comparisons and implications *Acta Geotech* **18**, 2615–37.

Pandit. B., Tiwari. G., Latha, G.M., Babu, G.L.S. 2018. Stability Analysis of a Large Gold Mine Open-Pit Slope Using Advanced Probabilistic Method *Rock Mech Rock Eng* **51**, 2153–74.

Xu, Z., Zhou, X., Qian, Q. 2020. The uncertainty importance measure of slope stability based on the moment-independent method *Stochastic Environmental Research and Risk Assessment* **34**, 51–65.

Zhang, J., Shields, M.D. 2018. On the quantification and efficient propagation of imprecise probabilities resulting from small datasets *Mech Syst Signal Process* **98**, 465–83.